



Concentrations and stable carbon isotope compositions of oxalic acid and related SOA in Beijing before, during, and after the 2014 APEC

Jiayuan Wang^{1,3}, Gehui Wang^{1,2,3,4}, Jian Gao^{5,6}, Han Wang^{5,6}, Yanqin Ren^{1,3}, Jianjun Li¹, Bianhong Zhou¹, Can Wu^{1,3}, Lu Zhang^{1,3}, Shulan Wang^{5,6}, and Fahe Chai^{5,6}

¹State Key Laboratory of Loess and Quaternary Geology, Key Lab of Aerosol Chemistry and Physics, Institute of Earth Environment, Chinese Academy of Sciences, Xi'an 710061, China

²School of Human Settlements and Civil Engineering, Xi'an Jiaotong University, Xi'an 710079, China

³University of Chinese Academy of Sciences, Beijing 100049, China

⁴Center for Excellence in Regional Atmospheric Environment, Institute of Urban Environment, Chinese Academy of Sciences, Xiamen 361021, China

⁵State Key Laboratory of Environmental Criteria and Risk Assessment, Chinese Research Academy of Environmental Sciences, Beijing 100084, China

⁶Collaborative Innovation Center of Atmospheric Environment and Equipment Technology, Nanjing 210000, China

Correspondence to: Gehui Wang (wanggh@ieecas.cn) and Jian Gao (gaojian@craes.org.cn)

Received: 22 July 2016 – Published in Atmos. Chem. Phys. Discuss.: 22 August 2016

Revised: 29 December 2016 – Accepted: 3 January 2017 – Published: 23 January 2017

Abstract. To ensure good air quality for the 2014 Asia-Pacific Economic Cooperation (APEC) summit, stringent emission controls were implemented in Beijing and its surrounding regions, leading to a significant reduction in PM_{2.5} loadings. To investigate the impact of the emission controls on aerosol chemistry, high-volume PM_{2.5} samples were collected in Beijing from 8 October to 24 November 2014 and determined for secondary inorganic aerosols (SIA, i.e., SO₄^{2−}, NO₃[−], and NH₄⁺), dicarboxylic acids, keto-carboxylic acid, and α -dicarbonyls, as well as stable carbon isotope composition of oxalic acid (C₂). Our results showed that SIA, C₂, and related secondary organic aerosols in PM_{2.5} during APEC were 2–4 times lower than those before APEC, which is firstly ascribed to the strict emission control measures and secondly attributed to the relatively colder and drier conditions during the event that are unfavorable for secondary aerosol production.

C₂ in the polluted air masses, which mostly occurred before APEC, are abundant and enriched in ¹³C. On the contrary, C₂ in the clean air masses, which mostly occurred during APEC, is much less abundant but still enriched in ¹³C. In the mixed type of clean and polluted air masses, which mostly occurred after APEC, C₂ is lower than that before

APEC but higher than that during APEC and enriched in lighter ¹²C. A comparison on chemical composition of fine particles and $\delta^{13}\text{C}$ values of C₂ in two events that are characterized by high loadings of PM_{2.5} further showed that after APEC SIA and the total detected organic compounds (TDOC) are much less abundant and fine aerosols are enriched with primary organics and relatively fresh, compared with those before APEC.

1 Introduction

Atmospheric aerosols profoundly impact the global climate directly by scattering and absorbing solar radiation and indirectly by affecting cloud formation and distribution via acting as cloud condensation nuclei (CCN) and ice nuclei (IN). Moreover, atmospheric aerosols exert negative effects on human health because of their toxicity. Due to fast urbanization and industrialization, high levels of atmospheric fine particle (PM_{2.5}) pollution have been a persistent problem in many cities of China since the 1990s (van Donkelaar et al., 2010). As the capital of China and one of the largest megacities in the world, Beijing has suffered from frequent severe

haze pollution, especially in winter, affecting more than 21 million people by the end of 2014 (Beijing Municipal Bureau of Statistics, 2015) and causing billions in economic losses (Mu and Zhang, 2013). To improve the air quality, the Beijing government has made many efforts to reduce the pollutant emissions (i.e., SO_2 , NO_x , dust, and volatile organic compounds (VOCs)) from a variety of sources. The 2014 Asia-Pacific Economic Cooperation (APEC) summit was hosted in Beijing from 5 to 11 November. To ensure good air quality for the summit, a joint strict emission control program was conducted from 3 November 2014 in Beijing and its neighboring provinces including Inner Mongolia, Shanxi, Hebei, and Shandong provinces. During this period thousands of factories and power plants with high emissions were shut down and/or halted, all the construction activities were stopped, and the numbers of on-road vehicles were reduced. These strict emission controls resulted in the air quality of Beijing during the APEC period being significantly improved, leading to a decrease in $\text{PM}_{2.5}$ concentration by 59.2 % and an increase in visibility by 70.2 % in Beijing during the summit compared with those before the APEC (Tang et al., 2015; Z. Wang et al., 2015) and a term of “APEC blue” being created to refer to the good air quality. Such strong artificial intervening not only reduced $\text{PM}_{2.5}$ and its precursors’ loadings in Beijing and its surrounding areas but also affected the composition and formation mechanisms of the fine particles (Sun et al., 2016).

A number of field measurements have shown that particle compositions in Beijing during wintertime haze periods are dominated by secondary aerosols (Guo et al., 2014; Huang et al., 2014; Xu et al., 2015). Rapid accumulation of particle mass in Beijing during the haze formation process is often accompanied by continuous particle size growth (Guo et al., 2014; Zhang et al., 2015), which is in part due to the coating of secondary organic aerosols (SOA) on pre-existing particles (Li et al., 2010). Several studies have found that SOA production during the 2014 Beijing APEC periods significantly reduced and ascribed this reduction to the efficient regional emission control (Sun et al., 2016; Xu et al., 2015). However, up to now information on the SOA decrease on a molecular level has not been reported.

Dicarboxylic acids are the major class of SOA species in the atmosphere and ubiquitously found from the ground surface to the free troposphere (Fu et al., 2008; Myriokefalitakis et al., 2011; Sorooshian et al., 2007; Sullivan and Prather, 2007). Previous studies have suggested that organic acids including dicarboxylic acids could take part in atmospheric particle nucleation (Zhang et al., 2004; Zhao et al., 2009) and growth processes (Zhang et al., 2012). Furthermore, organic acids may play a central role in the aging of black carbon particles (Xue et al., 2009; Ma et al., 2013), enhancing their roles in air pollution accumulation, and direct radiative forcing (Peng et al., 2016). In the current work we measured molecular distributions of dicarboxylic acids, keto-carboxylic acids and α -dicarbonyls and stable carbon

isotope composition of oxalic acid in $\text{PM}_{2.5}$ aerosols collected in Beijing before, during, and after the APEC event in order to explore the impact of the APEC emission control on SOA in Beijing. We first investigated the changes in concentration and composition of dicarboxylic acids and related compounds during the three periods, then recognized the difference in stable carbon isotope composition of oxalic acid in different air masses in Beijing during the APEC campaign. Finally we compared the differences in chemical compositions of $\text{PM}_{2.5}$ during two heaviest pollution episodes.

2 Experimental section

2.1 Sample collection

$\text{PM}_{2.5}$ samples were collected by using a high-volume sampler (TISCH, USA) from 8 October to 24 November 2014 on the rooftop of a three-storey building located on the campus of the China Research Academy of Environmental Sciences, which is situated in the north part of Beijing and close to the fifth ring road. All the $\text{PM}_{2.5}$ samples were collected onto pre-baked (450 °C for 8 h) quartz fiber filters (Whatman 41, USA). The duration of each sample collection is 23 h from 08:00 LT of the previous day to 07:00 LT of the next day. Field blanks were also collected before and after the campaign by mounting a pre-baked filter onto the sampler for 15 min without pumping air. After collection, all the filter samplers were individually sealed in aluminum foil bags and stored in a freezer (−18 °C) prior to analysis. Daily values of SO_2 , NO_x , and meteorological parameters were cited from the website of Beijing Environmental Protection Agency.

2.2 Sample analysis

2.2.1 Elemental carbon (EC), organic carbon (OC), water-soluble organic carbon (WSOC), inorganic ions, aerosol liquid water content (ALWC) and aerosol acidity

Detailed methods for the analysis of EC, OC, WSOC, and inorganic ions in aerosols were reported elsewhere (Wang et al., 2010). Briefly, EC and OC in the $\text{PM}_{2.5}$ samples were determined by using DRI Model 2001 Carbon analyzer following the Interagency Monitoring of Protected Visual Environments (IMPROVE) thermal/optical reflectance (TOR) protocol (Chow et al., 2007). WSOC and inorganic ions in the samples were extracted with Milli-Q pure water and measured by using a Shimadzu TOC-L CPH analyzer and Dionex-600 ion chromatography, respectively (Wang et al., 2010). In the current work, aerosol liquid water content (ALWC) and acidity (i.e., liquid H^+ concentrations, $[\text{H}^+]$) of the samples were calculated by using ISORROPIA-II model, which treated the $\text{Na}^+ - \text{NH}_4^+ - \text{K}^+ - \text{Ca}^{2+} - \text{Mg}^{2+} - \text{Cl}^- - \text{NO}_3^- - \text{SO}_4^{2-}$ system (Hennigan et al., 2015; Weber et al., 2016).

Table 1. Meteorological parameters and concentrations of gaseous pollutants and chemical components of PM_{2.5} in Beijing during the 2014 APEC campaign.

	Whole period (<i>N</i> = 48)	Before APEC (08/10–02/11) (<i>N</i> = 26)	During APEC (03/11–12/11) (<i>N</i> = 10)	After APEC (13/11–14/11) (<i>N</i> = 12)
I. Meteorological parameters				
Temperature, °C	9.5 ± 4.3 (3.0–18)	13 ± 2.6 (9.0–18)	7.0 ± 1.7 (4.0–10)	4.3 ± 1.3 (3.0–7.0)
Relative humidity, %	56 ± 19 (17–88)	62 ± 19 (22–88)	47 ± 14 (17–65)	51 ± 16 (29–80)
Visibility, km	8.8 ± 6.8 (1.0–28)	7.3 ± 6.6 (1.0–24)	13 ± 7.7 (6.0–28)	7.2 ± 4.2 (2.0–15)
Wind speed, km h ^{−1}	8.0 ± 4.9 (3.0–26)	7.6 ± 4.8 (3.0–26)	9.4 ± 6.6 (3.0–26)	7.8 ± 2.9 (3.0–13)
II. Gaseous pollutants, µg m ^{−3}				
O ₃	48 ± 23 (6.0–115)	55 ± 24 (9.0–115)	52 ± 13 (25–69)	29 ± 18 (6.0–60)
SO ₂	12 ± 8.5 (2.0–43)	8.8 ± 4.6 (2.0–19)	7.6 ± 3.9 (2.0–15)	23 ± 8.8 (13–43)
NO ₂	68 ± 29 (10–135)	71 ± 27 (22–118)	45 ± 18 (10–69)	78 ± 29 (45–135)
CO	1360 ± 730 (220–3320)	1370 ± 700 (250–2460)	960 ± 410 (220–1420)	1720 ± 830 (740–3320)
III. Major components of PM _{2.5} , µg m ^{−3}				
PM _{2.5}	157 ± 110 (16–408)	178 ± 122 (16–408)	98 ± 46 (28–183)	161 ± 100 (36–383)
SO ₄ ^{2−}	12 ± 11.5 (1.2–43)	15 ± 13 (1.2–43)	5.3 ± 2.8 (1.8–11)	11 ± 10 (2.9–34)
NO ₃ [−]	21 ± 22 (0.32–88)	28 ± 26 (0.32–88)	10 ± 8.1 (1.2–26)	15 ± 13 (2.9–46)
NH ₄ ⁺	7.3 ± 7.2 (0.2–28)	9.0 ± 8.0 (0.2–28)	3.1 ± 2.6 (0.2–8.6)	6.9 ± 6.4 (1.0–22)
OC ^a	28 ± 18 (5.7–78)	26 ± 16 (6.0–67)	19 ± 7.6 (5.7–29)	39 ± 23 (9.7–78)
EC ^a	8.8 ± 5.4 (1.4–25)	8.6 ± 4.6 (1.4–18)	6.0 ± 2.7 (1.5–9.6)	12 ± 7.0 (2.1–25)
WSOC ^b	10 ± 6.0 (2.4–32)	11 ± 4.6 (3.1–32)	6.4 ± 2.6 (2.4–11)	11 ± 6.1 (4.5–24)
ALWC ^c	40 ± 62 (0–299)	58 ± 75 (0–299)	6.3 ± 5.5 (0–19)	28 ± 41 (0.4–136)
[H ⁺] ^d	0.083 ± 0.14 (0–0.56)	0.13 ± 0.17 (0–0.56)	0.026 ± 0.025 (0–0.072)	0.033 ± 0.067 (0–0.20)
IV. Mass ratios of major components of PM _{2.5}				
NO ₃ [−] / SO ₄ ^{2−}	1.6 ± 0.8 (0.3–4.3)	1.7 ± 0.9 (0.3–4.3)	1.6 ± 0.7 (0.5–2.4)	1.4 ± 0.4 (0.8–2.2)
OC / EC	3.3 ± 0.6 (2.2–4.7)	3.2 ± 0.7 (2.2–4.5)	3.3 ± 0.6 (2.0–4.3)	3.4 ± 0.5 (2.7–4.7)
WSOC / OC	0.39 ± 0.15 (0.10–0.71)	0.42 ± 0.13 (0.13–0.71)	0.38 ± 0.16 (0.16–0.65)	0.35 ± 0.17 (0.10–0.63)

^a Organic carbon (OC) and elemental carbon (EC). ^b Water-soluble organic carbon (WSOC). ^c Aerosol liquid water content (ALWC). ^d Hydrogen ion concentration ([H⁺]).

2.2.2 Dicarboxylic acids, keto-carboxylic acids and α-dicarbonyls

The method of analyzing PM_{2.5} samples for dicarboxylic acids, ketocarboxylic acids and α-dicarbonyl has been reported elsewhere (Wang et al., 2002, 2012; Meng et al., 2014; Cheng et al., 2015). Briefly, one eighth of the filter was extracted with Milli-Q water, concentrated to near dryness, and reacted with 14 % BF₃/butanol at 100 °C for 1 h to convert the aldehyde group into dibutoxy acetal and the carboxyl group into butyl ester. Target compounds in the derivatized samples were identified by gas chromatography–mass spectrometry (GC–MS) and quantified by a gas chromatography–flame ionization detector (GC–FID) (Agilent GC7890A).

2.3 Stable carbon isotope composition of oxalic acid (C₂)

Stable carbon isotope composition (δ¹³C) of C₂ was measured using the method developed by Kawamura and Watanabe (2004). Briefly, δ¹³C values of the derivatized samples above were determined by gas chromatography–isotope ratio mass spectrometry (GC–IR–MS; Thermo Fisher, Delta V Advantage). The δ¹³C value of C₂ was then calculated from an isotopic mass-balance equation based on the measured δ¹³C of the derivatizations and the derivatizing reagent (1-butanol; Kawamura and Watanabe, 2004). Each sample was measured three times to ensure the difference of the δ¹³C values less than 0.2 ‰, and the isotope data reported here are the averaged value of the triplicate measurements.

Table 2. Concentrations of dicarboxylic acids and related compounds in PM_{2.5} in Beijing during the 2014 APEC campaign (ng m⁻³).

	Whole period (<i>N</i> = 48)	Before APEC (08/10–02/11) (<i>N</i> = 26)	During APEC (03/11–12/11) (<i>N</i> = 10)	After APEC (13/11–14/11) (<i>N</i> = 12)
I. Dicarboxylic acids				
Oxalic, C ₂	334 ± 461 (10–2127)	502 ± 564 (10.5–2127)	101 ± 69 (35–251)	166 ± 157 (22–554)
Malonic, C ₃	31 ± 42 (ND ^a –247)	45.7 ± 52.1 (1.44–247)	12 ± 8.0 (3.4–22.8)	16 ± 10.9 (ND–36)
Succinic, C ₄	74 ± 118 (3.0–722)	111 ± 150 (3.0–722)	24 ± 14 (7.1–42)	36 ± 26 (4.9–90)
Glutaric, C ₅	8.7 ± 12 (ND–68)	13 ± 15 (ND–68.1)	2.9 ± 2.24 (0.9–5.8)	4.9 ± 4.2 (ND–13)
Adipic, C ₆	13 ± 14 (0.9–83)	17 ± 18 (1.9–83)	5.9 ± 3.8 (2.1–14)	9.9 ± 7.1 (2.0–23)
Pimelic, C ₇	2.1 ± 3.8 (ND–27)	2.6 ± 5.1 (ND–27)	1.1 ± 0.7 (0.2–2.3)	2.0 ± 1.1 (0.9–4.4)
Suberic, C ₈	10 ± 11 (ND–66)	12 ± 13 (ND–66)	7.6 ± 5.0 (1.3–16)	8.7 ± 6.0 (2.0–21)
Azelaic, C ₉	5.0 ± 4.9 (0.5–21)	6.4 ± 5.7 (0.6–21)	1.7 ± 0.9 (0.5–3.2)	4.6 ± 3.3 (1.3–13)
Sebacic, C ₁₀	7.7 ± 7.4 (ND–34)	9.4 ± 8.8 (ND–34)	4.2 ± 3.6 (0.5–11)	6.8 ± 4.9 (1.4–16)
Undecanedioic, C ₁₁	11 ± 13 (ND–77)	14 ± 16 (ND–77)	3.3 ± 2.5 (ND–7.5)	9.4 ± 6.4 (0.8–23)
Methylsuccinic, iC ₅	13 ± 16 (0.6–79)	18 ± 19 (0.6–79)	4.8 ± 3.0 (1.0–9.2)	8.4 ± 6.0 (2.3–19)
Methylglutaric, iC ₆	7.5 ± 10 (ND–36)	11 ± 12 (ND–36)	0.9 ± 0.9 (ND–2.6)	4.6 ± 5.1 (ND–14)
Maleic, M	3.4 ± 3.9 (ND–15)	4.6 ± 4.7 (ND–15)	1.4 ± 0.8 (ND–2.9)	2.4 ± 2.0 (ND–6.3)
Fumaric, F	7.2 ± 8.8 (ND–64)	10 ± 11 (ND–64)	2.2 ± 1.5 (ND–5.4)	4.7 ± 3.2 (1.4–10)
Phthalic, Ph	17 ± 14 (1.5–64)	20 ± 16 (1.5–64)	10 ± 6.8 (2.3–20)	17 ± 9.0 (6.4–31)
Isophthalic, iPh	2.1 ± 2.5 (ND–10)	2.9 ± 2.8 (ND–10)	2.0 ± 2.1 (0.2–5.9)	0.5 ± 0.3 (ND–3.2)
Terephthalic, tPh	46 ± 35 (2.6–133)	50 ± 35 (2.6–123)	28 ± 19 (4.7–59)	53 ± 40 (7.4–133)
Subtotal	593 ± 739 (25–3788)	849 ± 905 (25–3788)	214 ± 135 (72–447)	354 ± 279 (85–965)
II. Keto-carboxylic acids				
Pyruvic, Pyr	24 ± 20 (1.3–84)	31 ± 23 (2.4–84)	15 ± 12 (1.3–36)	15 ± 9.3 (3.2–33)
Glyoxylic, ωC ₂	33 ± 51 (1.2–300)	48 ± 64 (1.2–300)	10 ± 7.7 (2.6–21)	20 ± 23 (2.8–80)
7-Oxoheptanoic, ωC ₇	8.8 ± 14 (ND–90)	13 ± 17 (ND–90)	4.2 ± 3.6 (ND–13)	4.5 ± 5.1 (ND–17)
Subtotal	66 ± 81 (3.6–474)	92 ± 99 (3.6–474)	30 ± 22 (5.9–66)	40 ± 35 (13–128)
III α-Dicarbonyls				
Glyoxal, Gly	44 ± 47 (4.2–270)	57 ± 56 (4.2–270)	22 ± 19 (4.9–47)	35 ± 30 (7.3–101)
Methylglyoxal, mGly	82 ± 82 (ND–406)	102 ± 96 (ND–406)	60 ± 52 (15–139)	58 ± 51 (5.8–144)
Subtotal	126 ± 115 (5.3–466)	158 ± 132 (5.3–466)	81.6 ± 67.4 (22–186)	93 ± 80 (14–225)
TDOC ^b	785 ± 872 (36–4636)	1099 ± 1104 (36–4636)	325 ± 220 (107–664)	487 ± 387 (117–1318)

^a ND: not detectable. ^b TDOC: total detected organic compounds.

3 Results and discussion

3.1 Variations in meteorological conditions, gaseous pollutants, and major components of PM_{2.5} during the Beijing 2014 APEC campaign

Based on the emission control implementation for the APEC, we divided the whole study period into three phases: before APEC (8 October to 2 November), during APEC (3 to 12 November) and after APEC (13 to 24 November). Temporal variations in meteorological parameters and concentrations of gaseous pollutants and major components of PM_{2.5} during the three phases are shown in Fig. 1 and summarized in Table 1.

Temperature during the sampling campaign showed a continuous decreasing trend with averages of 13 ± 2.6, 7.0 ± 1.7, and 4.3 ± 1.3 °C before, during, and after APEC, respec-

tively, while relative humidity (RH) did not show a clear trend, with mean values of 62 ± 19, 47 ± 14, and 51 ± 16 % during the three periods (Fig. 1a and Table 1). SO₂ showed a similar level before and during APEC (8.8 ± 4.6 μg m⁻³ versus 7.6 ± 3.9 μg m⁻³; Table 1 and Fig. 1b), but increased dramatically to 23 ± 8.8 μg m⁻³ after APEC due to domestic coal burning for house heating. NO₂ concentration (45 ± 18 μg m⁻³) during the APEC reduced by about 30 % compared to that in the before- and after-APEC phases (71 ± 27 μg m⁻³ versus 78 ± 29 μg m⁻³; Table 1), mainly because of the reduction of the on-road vehicle numbers, as well as the reduced productivities of power plant and industry. O₃ displayed a decreasing trend similar to that of temperature (Fig. 1c). PM_{2.5} pollution episodes in Beijing showed a periodic cycle of 4–5 days, which is caused by the local weather cycles. Secondary inorganic aerosols (SIA,

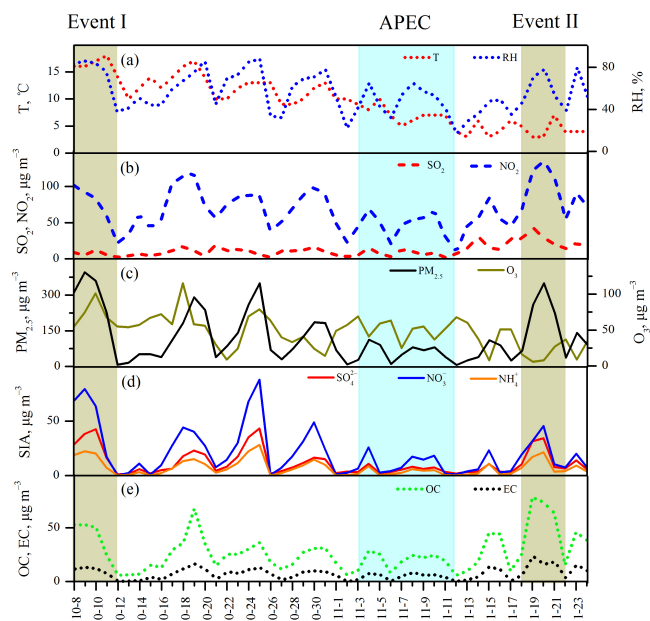


Figure 1. Temporal variations of meteorological conditions, gaseous pollutants and major components of $\text{PM}_{2.5}$ during the 2014 APEC campaign. (The green shadows represent two air pollution events characterized by highest $\text{PM}_{2.5}$ levels before and after APEC, while the blue shadow represents the APEC event).

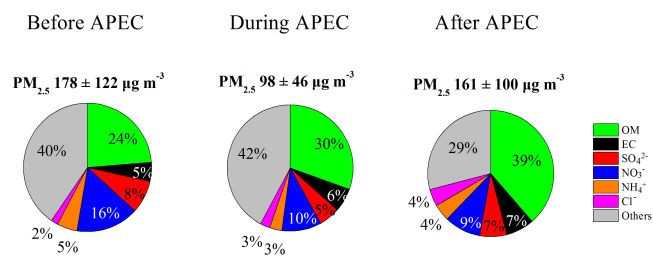


Figure 2. Chemical composition of $\text{PM}_{2.5}$ during the 2014 APEC campaign.

i.e., SO_4^{2-} , NO_3^- , and NH_4^+) are major components of $\text{PM}_{2.5}$ and present a temporal variation pattern similar to that of the fine particles (Fig. 1d). In the current work, the mass ratio of $\text{NO}_3^- / \text{SO}_4^{2-}$ in $\text{PM}_{2.5}$ during the whole study time is 1.8 ± 1.9 (Table 1), which is in agreement with the ratio (1.6–2.4) for PM_1 observed during the same time by using aerosol mass spectrometry (AMS; Sun et al., 2016). OC and EC of $\text{PM}_{2.5}$ are linearly correlated each other ($R^2 = 0.91$) and varied periodically in a cycle similar to SIA (Fig. 1e). The OC / EC ratio during the whole sampling period is 3.3 ± 0.6 (range: 2.2–4.7) with no significant differences among the three APEC phases (Table 1), although the source emissions could be largely different.

Figure 2 shows the differences in chemical composition of $\text{PM}_{2.5}$ before, during, and after APEC. $\text{PM}_{2.5}$ is $98 \pm 46 \mu\text{g m}^{-3}$ during APEC, about 50 % lower than

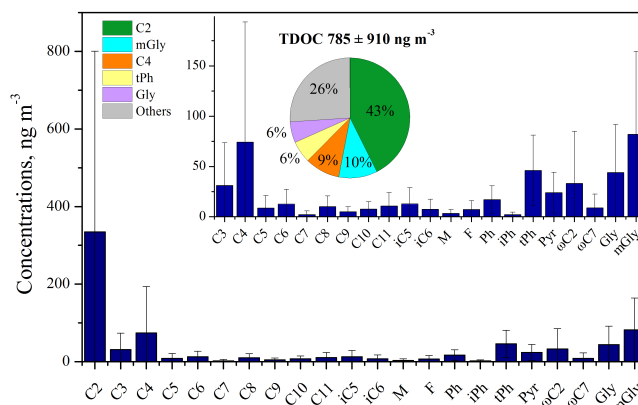


Figure 3. Molecular distributions of dicarboxylic acids and related compounds in $\text{PM}_{2.5}$ of Beijing, China, during the 2014 APEC campaign. The pie chart is the average composition of total detected organic compounds (TDOC) and the top number is the average mass concentration of TDOC of the whole study period.

that before and after APEC ($178 \pm 122 \mu\text{g m}^{-3}$ versus $161 \pm 100 \mu\text{g m}^{-3}$, respectively). Organic matter (OM) is the most abundant component of the fine particles. Relative abundance of OM (1.6 times OC; Xing et al., 2013) to $\text{PM}_{2.5}$ continuously increases from 24 % before APEC to 30 and 39 % during and after APEC, respectively, although the mass concentration ($19 \pm 7.6 \mu\text{g m}^{-3}$) of OC during APEC is the lowest compared to those before and after APEC ($26 \pm 16 \mu\text{g m}^{-3}$ versus $39 \pm 23 \mu\text{g m}^{-3}$). Sulfate, nitrate, and ammonium before APEC are 15 ± 13 , 28 ± 26 , and $9.0 \pm 8.0 \mu\text{g m}^{-3}$ (Table 1) and account for 8, 16, and 5 % of $\text{PM}_{2.5}$, respectively (Fig. 2). Their concentrations decrease to 5.3 ± 2.8 , 10 ± 8.1 , and $3.1 \pm 2.6 \mu\text{g m}^{-3}$ (Table 1) with the relative contributions to $\text{PM}_{2.5}$ down to 5, 10, and 3 % during APEC, respectively, while after APEC their concentrations increased to 11 ± 10 , 15 ± 13 , and $6.9 \pm 6.4 \mu\text{g m}^{-3}$ and accounted for 7, 9, and 4 % of $\text{PM}_{2.5}$. Such significant decreases in concentrations of OM and SIA during APEC demonstrate the efficiency of the emission controls. The OC / EC ratio is almost constant during the whole period, but the WSOC / OC ratio decreased by 20 % from 0.42 ± 0.13 before APEC, 0.38 ± 0.16 during APEC to 0.35 ± 0.17 after APEC (Table 1). Since WSOC in fine aerosols consists mainly of SOAs (Laskin et al., 2015), the decreasing ratio of WSOC / OC probably indicates reduced SOA production during the campaign.

3.2 Oxalic acid and related SOA during the Beijing 2014 APEC campaign

A homogeneous series of dicarboxylic acids (C_2 – C_{11}), keto-carboxylic acid and α -dicarbonyls in the $\text{PM}_{2.5}$ samples were detected. As shown in Table 2, total dicarboxylic acids during the whole study period is $593 \pm 739 \text{ ng m}^{-3}$, which is lower than that observed during the Campaign of Air Quality Re-

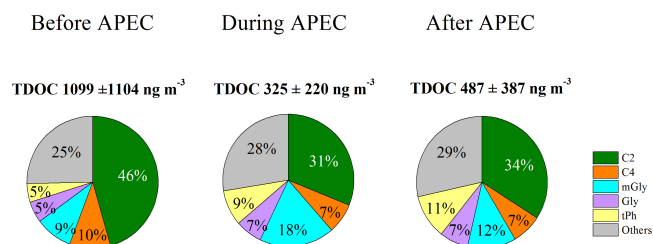


Figure 4. Compositions of total detected organic compounds (TDOC) in PM_{2.5} during the 2014 APEC campaign.

search in Beijing 2006 (CAREBeijing; average 760 ng m⁻³) and 2007 (average 1010 ng m⁻³; Ho et al., 2010, 2015) and the averaged wintertime concentration reported by a previous study on 14 Chinese cities (904 ng m⁻³; Ho et al., 2007). Total keto-carboxylic acid is 66 ± 81 ng m⁻³, while total dicarbonyl is 126 ± 115 ng m⁻³ (Table 2). These values are higher than those during CAREBeijing 2006 and 2007 (Ho et al., 2010, 2015), but close to the value observed for the 14 Chinese megacities (Ho et al., 2007). Being similar to those previous observations, oxalic acid (C₂) is the most abundant diacid in the 2014 APEC samples, with an average of 334 ± 461 ng m⁻³ (range: 10–2127 ng m⁻³, Table 2) during the whole campaign, followed by methylglyoxal (mGly), succinic acid (C₄), terephthalic acid (tPh), and glyoxal (Gly). These five species account for 43, 10, 9, 6 and 6 % of total detected organic compounds (TDOC), respectively (Fig. 3).

As seen in Fig. 4, TDOC in PM_{2.5} are 1099 ± 1104, 325 ± 220, and 487 ± 387 ng m⁻³ before, during, and after APEC, respectively. In comparison with those before APEC, TDOC during APEC decreased by 71 %. Oxalic acid (C₂) is the leading species among the detected organic compounds and accounted for 46, 31, and 34 % of TDOC during the three phases, respectively (Fig. 4). C₂ is an end product of precursors that are photochemically oxidized in aerosol aqueous phase via either oxidation of small compounds containing two carbon atoms or decomposition of larger compounds containing three or more carbon atoms. Thus the mass ratio of C₂ to TDOC is indicative of aerosol aging (Wang et al., 2012; Ho et al., 2015). As shown in Fig. 4, the highest proportion of C₂ before APEC suggests that organic aerosols during this period are more oxidized, compared to those during and after APEC. Gly and methylglyoxal (mGly) are the precursors of C₂. Mass ratios of both compounds to TDOC are lowest before APEC (Fig. 4), further indicating enhanced SOA production during this period.

3.3 Formation mechanism of oxalic acid

3.3.1 Correlation of oxalic acid with temperature, relative humidity (RH), aerosol liquid water content (ALWC) and acidity and sulfate

A few studies have pointed out that aerosol aqueous phase oxidation is a major formation pathway for oxalic acid (Yu et al., 2005; van Pinxteren et al., 2014; Bikkina et al., 2015; Tilgner and Herrmann, 2010). To explore the formation mechanism of oxalic acid, we calculated ALWC and acidity (i.e., proton concentration, [H⁺]) of PM_{2.5} aerosols by using ISOROPPIA-II model (Weber et al., 2016). As shown in Fig. 5, during the entire period C₂ showed a strong linear correlation with sulfate ($R^2 = 0.70$ Fig. 5a), which is consistent with the measurements observed in Xi'an (Wang et al., 2012) and other Chinese cities (Yu et al., 2005). Previous studies on particle morphology showed that sulfate particles internally mix with SOA in Beijing, especially on humid haze days (Li et al., 2010, 2011), which probably indicates that they are formed via similar aqueous phase pathways (Wang et al., 2016b). In addition, a robust correlation was also found for C₂ with RH ($R^2 = 0.64$, Fig. 5b) and ALWC ($R^2 = 0.61$, Fig. 5c), indicating that humid conditions are favorable for the aqueous phase formation of C₂, which is most likely due to an enhanced gas-to-aerosol aqueous phase partitioning of the precursors (e.g., Gly and mGly; Fu et al., 2008; G. Wang et al., 2015).

NH₄⁺, NO₃⁻, and SO₄²⁻ are the dominant cation and anions of fine particles in Beijing (Guo et al., 2014; Zhang et al., 2015) and the molar ratio of [NH₄⁺] to [NO₃⁻] + [SO₄²⁻] in this study is 1.1. Thus it is plausible that SO₄²⁻ during the APEC campaign largely existed as ammonium bisulfate, resulting in a strong linear correlation between [H⁺] and SO₄²⁻ with a molar slope of 1.03 (Fig. 5d; Zhang et al., 2007). In addition, [H⁺] shows a significant positive correlation with C₂ ($R^2 = 0.84$; Fig. 5e), possibly due to the fact that acidic conditions are favorable for the formation of C₂ precursors. For example, Surratt et al. (2007, 2010) found that aerosol acidity can promote the formation of biogenic SOA (BSOA) derived from isoprene oxidation, such as 2-methylglyceric acid, Gly and mGly. These BSOA precursors can be further oxidized into C₂ (Meng et al., 2014; Wang et al., 2009).

There is a significant positive correlation ($R^2 = 0.58$, $p < 0.001$) between the mass ratios of C₂ / TDOC and ambient temperatures (Fig. 5f), which is similar to the results found by previous researchers (Ho et al., 2007; Strader et al., 1999), indicating that organic aerosols are more aged under a higher temperature condition (Erven et al., 2011; Carlton et al., 2009). Thus, compared with those before APEC, the lower C₂ / TDOC ratios (31 and 34 % (Fig. 4) during and after APEC respectively) can be ascribed in part to the relatively lower temperature conditions that are not favorable for oxidation of the precursors to produce oxalic acid (13 ± 2.6,

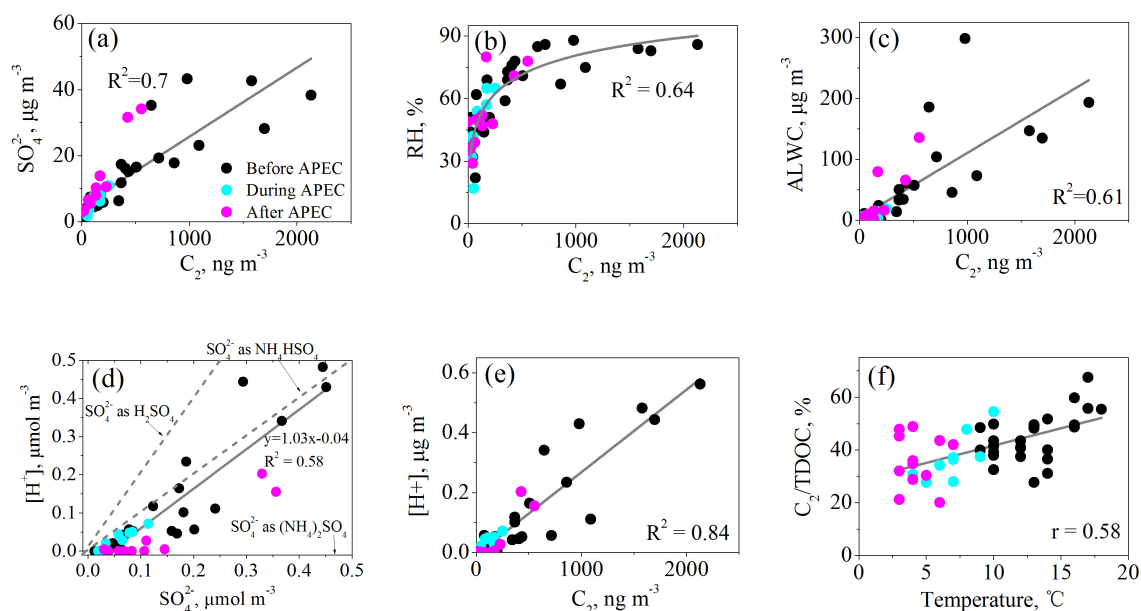


Figure 5. Correlation analysis for oxalic acid (C_2) and sulfate in $PM_{2.5}$ during the whole 2014 APEC campaign. (a–c) Concentrations of C_2 with sulfate, relative humidity (RH), and aerosol liquid water content (ALWC); (d, e) sulfate and C_2 with aerosol acidity $[H^+]$ and (f) temperature with mass ratio of C_2 to total detected organic compounds (C_2 / TDOC).

Table 3. Linear correlation coefficients of $\delta^{13}C$ of C_2 with $C_2 / \omega C_2$, $C_2 / mGly$, and TDOC / WSOC.

	$C_2 / \omega C_2$	$C_2 / mGly$	TDOC / WSOC
$\delta^{13}C$	0.49**	0.35*	0.41*

** $p < 0.01$; * $p < 0.05$.

7.0 ± 1.7 and 4.3 ± 1.3 °C in the before-, during- and after-APEC periods, respectively; Table 1).

3.3.2 Temporal variation in stable carbon isotopic composition of oxalic acid

To further discuss the formation mechanism of C_2 , we investigated the temporal variations of concentration and stable carbon isotopic composition of C_2 in the $PM_{2.5}$ samples (Fig. 6). Previous studies have demonstrated that Gly, mGly, glyoxylic acid (ωC_2), and pyruvic acid (Pyr) are the precursors of C_2 (Carlton et al., 2006, 2007; Ervens et al., 2004; Wang et al., 2012). Thus, higher mass ratios of C_2 to its precursors indicate that organic aerosols are more oxidized (Wang et al., 2010). As shown in Table 3, $\delta^{13}C$ of C_2 in this work positively correlated with the mass ratios of $C_2 / \omega C_2$, $C_2 / mGly$, and TDOC / WSOC, demonstrating an enrichment of ^{13}C during the aerosol oxidation process. Because decomposition (or breakdown) of larger molecular weight precursors in aerosol aqueous phase is the dominant formation pathway for C_2 in the aerosol ageing process (Kawamura

et al., 2016; Gensch et al., 2014; Kirillova et al., 2013), during which organic compounds release CO_2 / CO by reaction with OH radical and other oxidants, resulting in the evolved species enriched with lighter isotope (^{12}C) and the remaining substrate enriched in ^{13}C due to kinetic isotope effects (KIE; Hoefs, 1997; Rudolph et al., 2002).

A 72 h backward trajectory analysis showed that air masses that moved to Beijing during the whole sampling period can roughly be categorized into three types (Fig. 6a; all trajectories during the entire study period can be found in the Supplement). (1) Polluted type, by which air masses originated inland and east coastal China and moved slowly into Beijing within 72 h from its southern regions, i.e., Henan, Shandong, and Jiangsu provinces. This type of air mass mostly occurred before APEC with high $PM_{2.5}$ concentrations. Air pollution has been widely distributed in the three provinces (Wei et al., 2016); thus aerosols transported by this type of air mass are of regional characteristics. (2) Mixed type, by which air masses originated from Mongolia and North China, and moved quickly into Hebei province and then turned back to Beijing. The air in Mongolia and North China was clean but polluted in Hebei province, which is adjacent to Beijing. This type of air mass is a mixture of clean and polluted air and is thus named mixed type. Since the resident time of the mixed type of air mass within Hebei province is very short, thus aerosols transported by this type of air mass are of local characteristics and relatively fresh. (3) Clean type, by which air masses originated from Siberia and moved rapidly into Beijing directly via long-range transport. Aerosols from the clean type of air masses are much

Table 4. Meteorological parameters and chemical compositions ($\mu\text{g m}^{-3}$) of two maximum $\text{PM}_{2.5}$ between two pollution episodes in Beijing.

	T ($^{\circ}\text{C}$)	RH (%)	V^{a} (km)	$\text{PM}_{2.5}$	OC	EC	SIA^{b}	TDOC^{c}
Event I (8/10–11/10, Before APEC)	16.7 ± 0.8	82 ± 4	1.5 ± 0.5	349 ± 57	45 ± 12	12 ± 2	106 ± 39	2749 ± 1357
Event II (18/11–21/11, After APEC)	4.5 ± 1.7	62 ± 13	3.5 ± 1.5	259 ± 102	60 ± 21	17 ± 6	60 ± 32	831 ± 400

^a V : visibility. ^b SIA : secondary inorganic aerosols (the sum of sulfate, nitrate, and ammonium). ^c TDOC : total detected organic compounds.

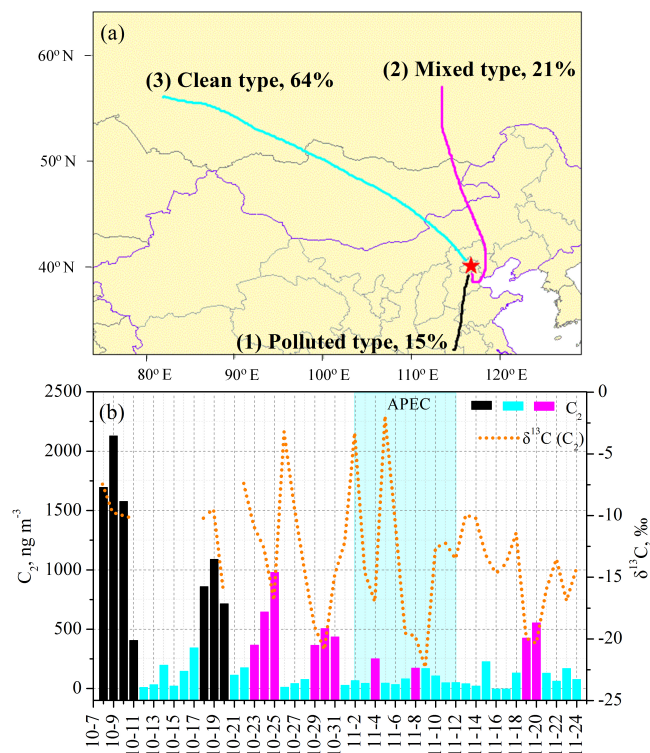


Figure 6. (a) 72 h backward trajectories determined by the National Oceanic and Atmospheric Administration Hybrid Single Particle Lagrangian Integrated Trajectory (HYSPPLIT) model arriving at the sampling site to reveal the major air-mass flow types during the study period. Northwestern wind (light blue) was most frequent (64 %), followed by northerly (21 %, pink) and southerly (15 %, black), and these are defined as clean, mixed, and polluted types, respectively (see the definitions in the text and the trajectories with a 6 h interval in the Supplement); (b) time series of $\delta^{13}\text{C}$ values and concentration of oxalic acid during the whole study period (colors in Fig. 6a are corresponding to those in Fig. 6b).

more aged, while those from the mixed type of air masses are fresh. Since severe air pollution is widespread in the southern regions, gas-to-aerosol phase partitioning of precursors and subsequent aerosol-phase oxidation to produce SOA including C_2 continuously proceed during the air-mass movement. However, such a partition for producing SOA is not significant when air masses move from Siberia, Mongolia, and

northern China because of the much less abundant VOCs. Instead, aerosols in the clean air masses are continuously oxidized, during which C_2 is produced by photochemical decomposition of larger molecular weight precursors. Therefore, C_2 in $\text{PM}_{2.5}$ transported by the mixed type air masses is not only fresh and abundant but also enriched in ^{12}C , whereas C_2 in $\text{PM}_{2.5}$ transported by the clean type air masses is aged, less abundant, and enriched in ^{13}C due to KIE effects, as illustrated by the pink and light blue columns in Fig. 6b, respectively. C_2 in $\text{PM}_{2.5}$ transported by the polluted type of air mass is most abundant compared with that in other two types of air mass, which is not only due to the severe air pollution in the Henan, Shandong, and Jiangsu provinces but also due to the enhanced photochemical oxidation under the humid, higher temperature and stagnant conditions that occurred mostly before APEC, as discussed previously. Therefore, C_2 in the polluted type of air masses is not only abundant but also enriched in ^{13}C (see black columns in Fig. 6b).

3.4 Different chemical characteristics of $\text{PM}_{2.5}$ between two severe haze events

From Fig. 1 and Table 4, it can be found that $\text{PM}_{2.5}$ showed two equivalent maxima on 9 October and 20 November during the whole study period. However, the chemical compositions of $\text{PM}_{2.5}$ during these two pollution events are significantly different. As shown in Fig. 7a, relative abundances of SIA (sum of SO_4^{2-} , NO_3^- , and NH_4^+) to $\text{PM}_{2.5}$ are 30 % during event I and 23 % during event II. The relative abundance of OM (21 %, Fig. 7a) during event I is lower than that (37 %) during event II (Fig. 7b). In contrast, the ratios of WSOC/OC and TDOC/OC are higher in event I than in event II, which is consistent with lower levels of O_3 after APEC (Table 1), suggesting a weaker photochemical oxidation capacity during event II. Organic biomarkers in the $\text{PM}_{2.5}$ samples have been measured for the source apportionment (Wang et al., 2016a) and cited here to further identify the difference in chemical composition of $\text{PM}_{2.5}$ between the two events. Levoglucosan is a key tracer for biomass burning smoke. The mass ratio of levoglucosan to OC in $\text{PM}_{2.5}$ (Lev/OC) is comparable between the two events, suggesting a similar level of contributions of biomass burning emission to $\text{PM}_{2.5}$ before and after APEC. However, the mass ratios of polycyclic aromatic hydrocarbons (PAHs) and

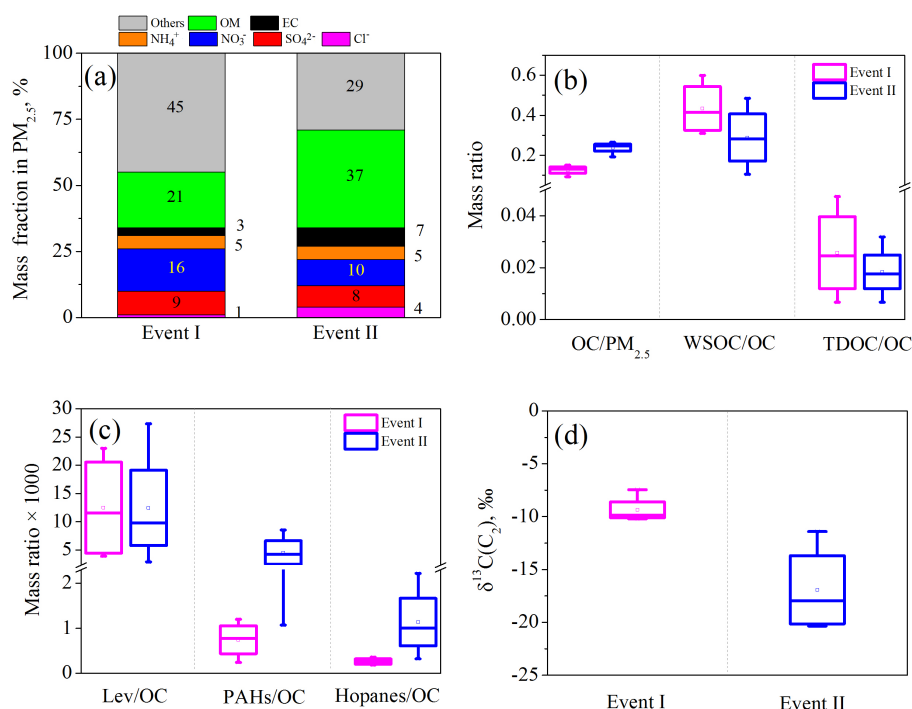


Figure 7. Comparison of chemical composition of PM_{2.5} during two air pollution events. **(a)** Percentages of major species in PM_{2.5}; **(b, c)** mass ratios of major species and organic tracers in PM_{2.5}; **(d)** stable carbon isotope composition of oxalic acid (C₂) (data about levoglucosan (Lev), PAHs, and hopanes are cited from Wang et al., 2016a).

hopanes to OC are lower in event I than those in event II (Fig. 7c), which again demonstrates the enhanced emissions from coal burning for house heating, because these compounds are key tracers of coal burning smokes (Wang et al., 2006). As seen in Fig. 7d, C₂ in event I was enriched in ¹³C. Such relatively more abundant SIA, WSOC, and TDOC and heavier C₂ in PM_{2.5} clearly demonstrate that PM_{2.5} during event I is enriched with secondary products while the fine particles during event II are enriched with primary compounds. After-APEC house heating activities including residential coal burning were activated, which emitted huge amounts of SO₂, NO_x, and VOCs as well as primary particles, resulting in both absolute concentrations and relative abundances of CO and EC 30–40 % higher after APEC than before APEC (see Table 1). Li et al. (2015) reported that VOCs in Beijing were 86 ppbv before APEC, 48 ppbv during APEC, and 73 ppbv after APEC. As shown in Table 4, temperature (16.7 ± 0.8 °C for event I and 4.5 ± 1.7 °C for event II) and relative humidity (RH; 82 ± 4 for event I and 62 ± 13 % for event II) are lower during event II than during event I. Moreover, air masses arriving in Beijing during event II are the mixed type, of which the resident time in Hebei province is short. Compared with those in event I, such colder and drier conditions and a short reaction time during event II are unfavorable for photochemical oxidation, resulting in SOA not only less abundant but also enriched with

lighter ¹²C during event II, although VOC levels are comparable before and after APEC.

4 Summary and conclusion

Temporal variations in molecular distribution of SIA, dicarboxylic acids, ketoacids, α-dicarbonyl, and stable carbon isotopic composition (δ¹³C) of C₂ in PM_{2.5} collected in Beijing before, during and after the 2014 APEC were investigated. Absolute concentrations and relative abundances of SIA and C₂ in PM_{2.5} are highest before APEC, followed by those after and during APEC, suggesting that the fine aerosols before APEC are enriched with secondary products, mainly due to an enhanced photochemical oxidation under the warm, humid and stagnant conditions. Concentrations of SIA, oxalic acid and related SOA in PM_{2.5} during APEC are 2–4 times lower than those before APEC, which can be ascribed to the effective emission controls and the favorable meteorological conditions that brought clean air from Siberia and Mongolia into Beijing.

Positive correlations of C₂ with sulfate mass, RH, ALWC, and aerosol acidity indicate that the C₂ formation pathway is involved in acid-catalyzed aerosol aqueous phase oxidation. SIA, C₂, and related SOA in the polluted types of air mass are abundant with C₂ enriched in ¹³C. On the contrary, those in the clean types of air mass are much less abundant, although

C₂ is also enriched in ¹³C. By comparing the chemical composition of PM_{2.5} and δ¹³C values of C₂ in two events that are characterized by the highest loadings of PM_{2.5} before and after APEC, we further found that compared with those before APEC fine aerosols after APEC are enriched with primary species and C₂ is depleted in heavier ¹³C, although SO₂, NO_x, and VOCs are abundant during the heating season, again demonstrating the important role of meteorological conditions in the secondary aerosol formation process, which are warmer, humid, and stagnant before APEC and result in secondary species being much more abundant than those during and after APEC.

The Supplement related to this article is available online at doi:10.5194/acp-17-981-2017-supplement.

Acknowledgement. This work was financially supported by the Strategic Priority Research Program of the Chinese Academy of Sciences (grant no. XDB05020401), the China National Natural Science Funds for Distinguished Young Scholars (grant no. 41325014), and the program from the National Nature Science Foundation of China (no. 41405122, 91544226 and 41375132).

Edited by: R. Zhang

Reviewed by: three anonymous referees

References

- Beijing Municipal Bureau of Statistics: available at: http://www.bjstats.gov.cn/tjsj/yjdsj/rk/2014/201511/t20151124_323864.html, 2015.
- Bikkina, S., Kawamura, K., and Miyazaki, Y.: Latitudinal distributions of atmospheric dicarboxylic acids, oxocarboxylic acids, and α-dicarbonyls over the western North Pacific: Sources and formation pathways, *J. Geophys. Res.-Atmos.*, 120, 5010–5035, doi:10.1002/2014jd022235, 2015.
- Carlton, A. G., Turpin, B. J., Lim, H.-J., Altieri, K. E., and Seitzinger, S.: Link between isoprene and secondary organic aerosol (SOA): Pyruvic acid oxidation yields low volatility organic acids in clouds, *Geophys. Res. Lett.*, 33, L06822, doi:10.1029/2005gl025374, 2006.
- Carlton, A. G., Turpin, B. J., Altieri, K. E., Seitzinger, S., Reff, A., Lim, H.-J., and Ervens, B.: Atmospheric oxalic acid and SOA production from glyoxal: Results of aqueous photooxidation experiments, *Atmos. Environ.*, 41, 7588–7602, doi:10.1016/j.atmosenv.2007.05.035, 2007.
- Carlton, A. G., Wiedinmyer, C., and Kroll, J. H.: A review of Secondary Organic Aerosol (SOA) formation from isoprene, *Atmos. Chem. Phys.*, 9, 4987–5005, doi:10.5194/acp-9-4987-2009, 2009.
- Cheng, C., Wang, G., Meng, J., Wang, Q., Cao, J., Li, J., and Wang, J.: Size-resolved airborne particulate oxalic and related secondary organic aerosol species in the urban atmosphere of Chengdu, China, *Atmos. Res.*, 161–162, 134–142, doi:10.1016/j.atmosres.2015.04.010, 2015.
- Chow, J. C., Watson, J. G., Chen, L.-W. A., Chang, M. O., Robinson, N. F., Trimble, D., and Kohl, S.: The IMPROVE_A temperature protocol for thermal/optical carbon analysis: maintaining consistency with a long-term database, *J. Air Waste Manage. Assoc.*, 57, 1014–1023, 2007.
- Ervens, B., Feingold, G., Frost, G. J., and Kreidenweis, S. M.: A modeling study of aqueous production of dicarboxylic acids: 1. Chemical pathways and speciated organic mass production, *J. Geophys. Res.-Atmos.*, 109, D15206, doi:10.1029/2003JD004387, 2004.
- Ervens, B., Turpin, B. J., and Weber, R. J.: Secondary organic aerosol formation in cloud droplets and aqueous particles (aqSOA): a review of laboratory, field and model studies, *Atmos. Chem. Phys.*, 11, 11069–11102, doi:10.5194/acp-11-11069-2011, 2011.
- Fu, T.-M., Jacob, D. J., Wittrock, F., Burrows, J. P., Vrekousis, M., and Henze, D. K.: Global budgets of atmospheric glyoxal and methylglyoxal, and implications for formation of secondary organic aerosols, *J. Geophys. Res.*, 113, D15303, doi:10.1029/2007jd009505, 2008.
- Gensch, I., Kiendler-Scharr, A., and Rudolph, J.: Isotope ratio studies of atmospheric organic compounds: Principles, methods, applications and potential, *Int. J. Mass Spectrom.*, 365–366, 206–221, doi:10.1016/j.ijms.2014.02.004, 2014.
- Guo, S., Hu, M., Zamora, M. L., Peng, J., Shang, D., Zheng, J., Du, Z., Wu, Z., Shao, M., Zeng, L., Molina, M. J., and Zhang, R.: Elucidating severe urban haze formation in China, *P. Natl. Acad. Sci. USA*, 111, 17373–17378, doi:10.1073/pnas.1419604111, 2014.
- Hennigan, C. J., Izumi, J., Sullivan, A. P., Weber, R. J., and Nenes, A.: A critical evaluation of proxy methods used to estimate the acidity of atmospheric particles, *Atmos. Chem. Phys.*, 15, 2775–2790, doi:10.5194/acp-15-2775-2015, 2015.
- Ho, K. F., Cao, J. J., Lee, S. C., Kawamura, K., Zhang, R. J., Chow, J. C., and Watson, J. G.: Dicarboxylic acids, ketocarboxylic acids, and dicarbonyls in the urban atmosphere of China, *J. Geophys. Res.*, 112, D22S27, doi:10.1029/2006jd008011, 2007.
- Ho, K. F., Lee, S. C., Ho, S. S. H., Kawamura, K., Tachibana, E., Cheng, Y., and Zhu, T.: Dicarboxylic acids, ketocarboxylic acids, α-dicarbonyls, fatty acids, and benzoic acid in urban aerosols collected during the 2006 Campaign of Air Quality Research in Beijing (CAREBeijing-2006), *J. Geophys. Res.*, 115, D19312, doi:10.1029/2009jd013304, 2010.
- Ho, K. F., Huang, R.-J., Kawamura, K., Tachibana, E., Lee, S. C., Ho, S. S. H., Zhu, T., and Tian, L.: Dicarboxylic acids, ketocarboxylic acids, α-dicarbonyls, fatty acids and benzoic acid in PM_{2.5} aerosol collected during CAREBeijing-2007: an effect of traffic restriction on air quality, *Atmos. Chem. Phys.*, 15, 3111–3123, doi:10.5194/acp-15-3111-2015, 2015.
- Hoefs, J. and Hoefs, J.: *Stable isotope geochemistry*, Springer, 1997.
- Huang, R. J., Zhang, Y., Bozzetti, C., Ho, K. F., Cao, J. J., Han, Y., Daellenbach, K. R., Slowik, J. G., Platt, S. M., Canonaco, F., Zotter, P., Wolf, R., Pieber, S. M., Bruns, E. A., Crippa, M., Ciarelli, G., Piazzalunga, A., Schwikowski, M., Abbaszade, G., Schnelle-Kreis, J., Zimmermann, R., An, Z., Szidat, S., Baltensperger, U., El Haddad, I., and Prevot, A. S.: High secondary aerosol contribution to particulate pollution during haze events in China, *Nature*, 514, 218–222, doi:10.1038/nature13774, 2014.

- Kawamura, K. and Watanabe, T.: Determination of stable carbon isotopic compositions of low molecular weight dicarboxylic acids and ketocarboxylic acids in atmospheric aerosol and snow samples, *Anal. Chem.*, 76, 5762–5768, 2004.
- Kawamura, K. and Bikkina, S.: A review of dicarboxylic acids and related compounds in atmospheric aerosols: Molecular distributions, sources and transformation, *Atmos. Res.*, 170, 140–160, doi:10.1016/j.atmosres.2015.11.018, 2016.
- Kirillova, E. N., Andersson, A., Sheesley, R. J., Kruså, M., Praveen, P. S., Budhavant, K., Safai, P. D., Rao, P. S. P., and Gustafsson, Ö.: ^{13}C - and ^{14}C -based study of sources and atmospheric processing of water-soluble organic carbon (WSOC) in South Asian aerosols, *J. Geophys. Res.-Atmos.*, 118, 614–626, doi:10.1002/jgrd.50130, 2013.
- Laskin, A., Laskin, J., and Nizkorodov, S. A.: Chemistry of Atmospheric Brown Carbon, *Chem. Rev.*, 115, 4335–4382, doi:10.1021/cr5006167, 2015.
- Li, J., Xie, S. D., Zeng, L. M., Li, L. Y., Li, Y. Q., and Wu, R. R.: Characterization of ambient volatile organic compounds and their sources in Beijing, before, during, and after Asia-Pacific Economic Cooperation China 2014, *Atmos. Chem. Phys.*, 15, 7945–7959, doi:10.5194/acp-15-7945-2015, 2015.
- Li, W. and Shao, L.: Mixing and water-soluble characteristics of particulate organic compounds in individual urban aerosol particles, *J. Geophys. Res.*, 115, D02301, doi:10.1029/2009jd012575, 2010.
- Li, W., Zhou, S., Wang, X., Xu, Z., Yuan, C., Yu, Y., Zhang, Q., and Wang, W.: Integrated evaluation of aerosols from regional brown hazes over northern China in winter: Concentrations, sources, transformation, and mixing states, *J. Geophys. Res.*, 116, D09301, doi:10.1029/2010jd015099, 2011.
- Ma, Y., Brooks, S. D., Vidaurre, G., Khalizov, A. F., Wang, L., and Zhang, R.: Rapid modification of cloud-nucleating ability of aerosols by biogenic emissions, *Geophys. Res. Lett.*, 40, 6293–6297, doi:10.1002/2013gl057895, 2013.
- Meng, J., Wang, G., Li, J., Cheng, C., Ren, Y., Huang, Y., Cheng, Y., Cao, J., and Zhang, T.: Seasonal characteristics of oxalic acid and related SOA in the free troposphere of Mt. Hua, central China: implications for sources and formation mechanisms, *Sci. Total Environ.*, 493, 1088–1097, doi:10.1016/j.scitotenv.2014.04.086, 2014.
- Mu, Q. and Zhang, S.: An evaluation of the economic loss due to the heavy haze during January 2013 in China, *China Environmental Science*, 33, 2087–2094, 2013.
- Myriokefalitakis, S., Tsigaridis, K., Mihalopoulos, N., Sciare, J., Nenes, A., Kawamura, K., Segers, A., and Kanakidou, M.: In-cloud oxalate formation in the global troposphere: a 3-D modeling study, *Atmos. Chem. Phys.*, 11, 5761–5782, doi:10.5194/acp-11-5761-2011, 2011.
- Peng, J., Hu, M., Guo, S., Du, Z., Zheng, J., Shang, D., Zamora, M. L., Zeng, L., Shao, M., and Wu, Y.-S.: Markedly enhanced absorption and direct radiative forcing of black carbon under polluted urban environments, *P. Natl. Acad. Sci USA*, 113, 4266–4271, 2016.
- Rudolph, J., Czuba, E., Norman, A., Huang, L., and Ernst, D.: Stable carbon isotope composition of nonmethane hydrocarbons in emissions from transportation related sources and atmospheric observations in an urban atmosphere, *Atmos. Environ.*, 36, 1173–1181, 2002.
- Sorooshian, A., Lu, M.-L., Brechtel, F. J., Jonsson, H., Feingold, G., Flagan, R. C., and Seinfeld, J. H.: On the Source of Organic Acid Aerosol Layers above Clouds, *Environ. Sci. Technol.*, 41, 4647–4654, doi:10.1021/es0630442, 2007.
- Strader, R., Lurmann, F., and Pandis, S. N.: Evaluation of secondary organic aerosol formation in winter, *Atmos. Environ.*, 33, 4849–4863, 1999.
- Sullivan, R. C. and Prather, K. A.: Investigations of the Diurnal Cycle and Mixing State of Oxalic Acid in Individual Particles in Asian Aerosol Outflow, *Environ. Sci. Technol.*, 41, 8062–8069, doi:10.1021/es071134g, 2007.
- Sun, Y., Wang, Z., Wild, O., Xu, W., Chen, C., Fu, P., Du, W., Zhou, L., Zhang, Q., Han, T., Wang, Q., Pan, X., Zheng, H., Li, J., Guo, X., Liu, J., and Worsnop, D. R.: “APEC Blue”: Secondary Aerosol Reductions from Emission Controls in Beijing, *Sci. Rep.*, 6, 20668, doi:10.1038/srep20668, 2016.
- Surratt, J. D., Lewandowski, M., Offenberg, J. H., Jaoui, M., Kleindienst, T. E., Edney, E. O., and Seinfeld, J. H.: Effect of acidity on secondary organic aerosol formation from isoprene, *Environ. Sci. Technol.*, 41, 5363–5369, 2007.
- Surratt, J. D., Chan, A. W., Eddingsaas, N. C., Chan, M., Loza, C. L., Kwan, A. J., Hersey, S. P., Flagan, R. C., Wennberg, P. O., and Seinfeld, J. H.: Reactive intermediates revealed in secondary organic aerosol formation from isoprene, *P. Natl. Acad. Sci USA*, 107, 6640–6645, 2010.
- Tang, G., Zhu, X., Hu, B., Xin, J., Wang, L., Munkel, C., Mao, G., and Wang, Y.: Impact of emission controls on air quality in Beijing during APEC 2014: lidar ceilometer observations, *Atmos. Chem. Phys.*, 15, 12667–12680, doi:10.5194/acp-15-12667-2015, 2015.
- Tilgner, A. and Herrmann, H.: Radical-driven carbonyl-to-acid conversion and acid degradation in tropospheric aqueous systems studied by CAPRAM, *Atmos. Environ.*, 44, 5415–5422, 2010.
- van Donkelaar, A., Martin, R. V., Brauer, M., Kahn, R., Levy, R., Verduzco, C., and Villeneuve, P. J.: Global Estimates of Ambient Fine Particulate Matter Concentrations from Satellite-Based Aerosol Optical Depth: Development and Application, *Environ. Health Persp.*, 118, 847–855, 10.1289/ehp.0901623, 2010.
- van Pinxteren, D., Neusüß, C., and Herrmann, H.: On the abundance and source contributions of dicarboxylic acids in size-resolved aerosol particles at continental sites in central Europe, *Atmos. Chem. Phys.*, 14, 3913–3928, doi:10.5194/acp-14-3913-2014, 2014.
- Wang, G., Niu, S., Liu, C., and Wang, L.: Identification of dicarboxylic acids and aldehydes of PM₁₀ and PM_{2.5} aerosols in Nanjing, China, *Atmos. Environ.*, 36, 1941–1950, 2002.
- Wang, G., Kawamura, K., Lee, S., Ho, K., and Cao, J.: Molecular, seasonal, and spatial distributions of organic aerosols from fourteen Chinese cities, *Environ. Sci. Technol.*, 40, 4619–4625, 2006.
- Wang, G., Kawamura, K., Umemoto, N., Xie, M., Hu, S., and Wang, Z.: Water-soluble organic compounds in PM_{2.5} and size-segregated aerosols over Mount Tai in North China Plain, *J. Geophys. Res.*, 114, D19208, doi:10.1029/2008jd011390, 2009.
- Wang, G., Xie, M., Hu, S., Gao, S., Tachibana, E., and Kawamura, K.: Dicarboxylic acids, metals and isotopic compositions of C and N in atmospheric aerosols from inland China: implications for dust and coal burning emission and secondary aerosol formation

- tion, *Atmos. Chem. Phys.*, 10, 6087–6096, doi:10.5194/acp-10-6087-2010, 2010.
- Wang, G., Kawamura, K., Cheng, C., Li, J., Cao, J., Zhang, R., Zhang, T., Liu, S., and Zhao, Z.: Molecular distribution and stable carbon isotopic composition of dicarboxylic acids, keto-carboxylic acids, and alpha-dicarbonyls in size-resolved atmospheric particles from Xi'an City, China, *Environ. Sci. Technol.*, 46, 4783–4791, doi:10.1021/es204322c, 2012.
- Wang, G., Cheng, C., Meng, J., Huang, Y., Li, J., and Ren, Y.: Field observation on secondary organic aerosols during Asian dust storm periods: Formation mechanism of oxalic acid and related compounds on dust surface, *Atmos. Environ.*, 113, 169–176, doi:10.1016/j.atmosenv.2015.05.013, 2015.
- Wang, G., Wang, J., Ren, Y., and Li, J.: Chemical characterization of organic aerosols from Beijing during the 2014 APEC, *Atmos. Res.*, in preparation, 2016a.
- Wang, G., Zhang, R., Gomez, M. E., Yang, L., Levy Zamora, M., Hu, M., Lin, Y., Peng, J., Guo, S., Meng, J., Li, J., Cheng, C., Hu, T., Ren, Y., Wang, Y., Gao, J., Cao, J., An, Z., Zhou, W., Li, G., Wang, J., Tian, P., Marrero-Ortiz, W., Secrest, J., Du, Z., Zheng, J., Shang, D., Zeng, L., Shao, M., Wang, W., Huang, Y., Wang, Y., Zhu, Y., Li, Y., Hu, J., Pan, B., Cai, L., Cheng, Y., Ji, Y., Zhang, F., Rosenfeld, D., Liss, P. S., Duce, R. A., Kolb, C. E., and Molina, M. J.: Persistent sulfate formation from London Fog to Chinese haze, *P. Natl. Acad. Sci USA*, 113, 13630–13635, doi:10.1073/pnas.1616540113, 2016b.
- Wang, Z., Li, Y., Chen, T., Li, L., Liu, B., Zhang, D., Sun, F., Wei, Q., Jiang, L., and Pan, L.: Changes in atmospheric composition during the 2014 APEC conference in Beijing, *J. Geophys. Res.-Atmos.*, 120, 12695–12707, doi:10.1002/2015JD023652, 2015.
- Weber, R. J., Guo, H., Russell, A. G., and Nenes, A.: High aerosol acidity despite declining atmospheric sulfate concentrations over the past 15 years, *Nat. Geosci.*, 9, 282–285, doi:10.1038/ngeo2665, 2016.
- Wei, X., Gu, X., Chen, H., Cheng, T., Wang, Y., Guo, H., Bao, F., and Xiang, K.: Multi-Scale Observations of Atmosphere Environment and Aerosol Properties over North China during APEC Meeting Periods, *Atmosphere*, 7, 4, doi:10.3390/atmos7010004, 2016.
- Xing, L., Fu, T.-M., Cao, J. J., Lee, S. C., Wang, G. H., Ho, K. F., Cheng, M.-C., You, C.-F., and Wang, T. J.: Seasonal and spatial variability of the OM/OC mass ratios and high regional correlation between oxalic acid and zinc in Chinese urban organic aerosols, *Atmos. Chem. Phys.*, 13, 4307–4318, doi:10.5194/acp-13-4307-2013, 2013.
- Xu, W. Q., Sun, Y. L., Chen, C., Du, W., Han, T. T., Wang, Q. Q., Fu, P. Q., Wang, Z. F., Zhao, X. J., Zhou, L. B., Ji, D. S., Wang, P. C., and Worsnop, D. R.: Aerosol composition, oxidation properties, and sources in Beijing: results from the 2014 Asia-Pacific Economic Cooperation summit study, *Atmos. Chem. Phys.*, 15, 13681–13698, doi:10.5194/acp-15-13681-2015, 2015.
- Xue, H., Khalizov, A. F., Wang, L., Zheng, J., and Zhang, R.: Effects of coating of dicarboxylic acids on the mass-mobility relationship of soot particles, *Environ. Sci. Technol.*, 43, 2787–2792, 2009.
- Yu, J. Z., Huang, X.-F., Xu, J., and Hu, M.: When Aerosol Sulfate Goes Up, So Does Oxalate? Implication for the Formation Mechanisms of Oxalate, *Environ. Sci. Technol.*, 39, 128–133, doi:10.1021/es049559f, 2005.
- Zhang, R., Suh, I., Zhao, J., Zhang, D., Fortner, E. C., Tie, X., Molina, L. T., and Molina, M. J.: Atmospheric new particle formation enhanced by organic acids, *Science*, 304, 1487–1490, doi:10.1126/science.1095139, 2004.
- Zhang, Q., Jimenez, J. L., Worsnop, D. R., and Canagaratna, M.: A case study of urban particle acidity and its influence on secondary organic aerosol, *Environ. Sci. Technol.*, 41, 3213–3219, 2007.
- Zhang, R., Khalizov, A., Wang, L., Hu, M., and Xu, W.: Nucleation and growth of nanoparticles in the atmosphere, *Chem. Rev.*, 112, 1957–2011, doi:10.1021/cr2001756, 2012.
- Zhang, R., Wang, G., Guo, S., Zamora, M. L., Ying, Q., Lin, Y., Wang, W., Hu, M., and Wang, Y.: Formation of urban fine particulate matter, *Chem. Rev.*, 115, 3803–3855, doi:10.1021/acs.chemrev.5b00067, 2015.
- Zhao, J., Khalizov, A., Zhang, R., and McGraw, R.: Hydrogen-bonding interaction in molecular complexes and clusters of aerosol nucleation precursors, *J. Phys. Chem. A*, 113, 680–689, 2009.